Model for photonuclear reactions at intermediate energies

M. Gari and H. Hebach

Institut für Theoretische Physik, Ruhr-Universität Bochum, Bochum, Germany
and Max-Planck-Institut für Chemie, Mainz, Germany
(Received 24 June 1974)

In the present paper we discuss photonuclear reactions for photon energies $E_\gamma > 50$ MeV. We show in detail how the different processes concerning the nucleon-nucleon interactions enter the transition matrix. Explanations are given for the similar behavior of (γ, n) and (γ, p) and for a strong relative suppression of the reactions (γ, pp) and (γ, nn) compared to (γ, np). This solves the standing problems of photonuclear reactions at intermediate photon energies. We present numerical calculations for the reactions (γ, p) and (γ, n) on ^{4}He from 50 to 140 MeV photon energy and show in detail how the different physical processes numerically enter the total cross sections and angular distributions. Over-all good agreement with the experiments is achieved.

$$\left[\text{NUCLEAR REACTIONS } {}^4\text{He}(\gamma, p), \; {}^4\text{He}(\gamma, n) \; E = 50\text{--}140 \text{ MeV; calculated } \sigma, \; \sigma(\theta). \right]$$

I. INTRODUCTION

Several attempts have been made for years to explain the cross sections and angular distributions of photonuclear reactions at intermediate energies. The description of processes like (γ, n), (γ, p), (γ, pn), (γ, pp), and (γ, nn) in the pure shell model is very unsatisfactory. Experimentally the cross sections for (γ, n) and (γ, p) as well as the angular distributions show very similar behavior. The cross section for (γ, pn) is relatively large while the reactions (γ, pp) and (γ, nn) are not very well known. The cross sections calculated in the shell model (sm) for (γ, n) and (γ, p) are too small by about one order of magnitude compared to the experiments.[1,2] Also, the angular distribution does not give the trend shown by the experiments; whereas the angular distributions for (γ, p) show the observed peak in forward direction, (γ, n) shows a peak in backward direction which is in contrast to the experiment. The reactions (γ, pn), (γ, pp), and (γ, nn) are not explainable at all. There were several attempts to go beyond the shell model calculations by introducing nucleon-nucleon correlations. Several methods have been used: (i) Jastrow type correlations,[2-4] (ii) short range correlations calculated in the Bethe-Goldstone formalism,[1] to name a few of them. The reactions (γ, pn) have been treated mainly in the quasideuteron model first introduced by Levinger.[5] The above mentioned calculations were only partially successful. Neither Jastrow correlations nor Bethe-Goldstone type calculations were able to give a satisfactory description of photonuclear reactions.

In the present paper we outline a method for the treatment of photonuclear reactions which avoids the shortcomings of the above mentioned methods. In going beyong the sm calculations we have to insure several points of consistency: (i) orthogonality of the wave functions, (ii) gauge invariance of our description of the process. The problem of gauge invariance is a very severe one as we have shown in an earlier paper.[6] Introducing correlations does imply that electromagnetic interactions coupled to the correlations also have to be considered in order to insure gauge invariance (Fig. 1).

In the present paper we start from the simplest possible description in going beyond the shell model. We introduce NN correlations by means of meson exchanges. This enables us to keep track of physical processes entering the reactions. We shall see that the gauge contributions to the introduced correlations will make up the most important part of the processes below pion threshold. This gives an explanation for the suppression of the reactions (γ, pp), (γ, nn) compared to (γ, nn). It gives also an explanation of the success of the quasideuteron model. Nucleon-nucleon correlations in the usual sense are shown not to be as important as expected from earlier calculations.

We shall present as a numerical example cross sections and angular distributions for the reactions (γ, p) and (γ, n) on ^{4}He. We show in detail the importance of the different contributions to these reactions. Although the calculations are done in the most simple way we obtain a satisfactory description of the processes in nearly every point. This is mostly due to the unimportance of the short range NN correlations as only these are not very well known.
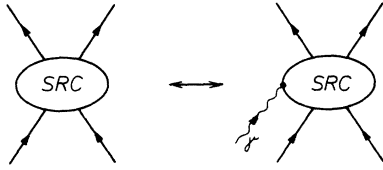
FIG. 1. Photonuclear correlations to be included together with the introduction of short-range correlations (SRC) for gauge reasons as far as electric transitions are concerned. For magnetic interactions these contributions do not follow from gauge arguments only.

II. TRANSITION MATRIX

The quantities of interest are the matrix elements for absorption of a photon of momentum k_γ (energy E_γ) while the nuclear system makes a transition from the state $|i\rangle = |1 \cdots A\rangle$ (only bound particles) to a state $|f\rangle = |(1 \cdots A - j)(j)\rangle$. Here j denotes the number of particles emitted from the nucleus after capture of the photon. We calculate the transition matrix

$$M_{fi} = \langle f | H_{el} | i \rangle, \tag{1}$$

where $H_{el} \equiv$ electromagnetic interaction, in a reference frame in which the total momentum is zero. In the following we are going to discuss the problems which arise in the calculation of the transition matrix. In order to achieve a deeper understanding of the physics of the reactions we are dealing with, we are going to keep apart all physical processes which enter the total transition matrix M_{fi}. We shall pay special attention to the question of how one can improve the calculations of a pure shell model. Going beyond the shell model treatment via inclusion of nucleon-nucleon correlations, one has to be aware of the fact that nucleon-nucleon correlations also have to be taken into account, which are coupled directly to the electromagnetic field (compare Fig. 1). We shall see that this type of process is of special importance for photonuclear reactions at intermediate energies. In the following we shall develop a model which takes into account in a consistent way nucleon-nucleon correlations and photomesonic interaction contributions. As the electric transitions are clearly dominating the photonuclear reactions we shall concentrate only on them. In connection with electric transitions we have to discuss the Siegert theorem which tells us that we do not have to worry about mesonic corrections. In view of this theorem one does not see immediately the reason for discussing mesonic exchange contributions to electric interactions. However, as we shall see in the following a much deeper understanding of photoreactions can be achieved by *not* using Siegert's theorem explicitly. Much more

can be learned by discussing the different processes which altogether make up the Siegert theorem.

In the absence of an electromagnetic field we start from a total nuclear Hamiltonian H_N in the form

$$H_N = T + V \tag{2}$$

with eigenvalues E_i and eigenstates $|\Psi_i\rangle$:

$$H_N | \Psi_i \rangle = E_i | \Psi_i \rangle . \tag{3}$$

As the many-body problem cannot be solved exactly we choose a shell model description

$$H_N = T + U + V - U \tag{4}$$

$$= H_0 + R; \quad R = V - U , \tag{5}$$

with eigenstates $|\Phi_i\rangle$ of the shell model Hamiltonian H_0:

$$H_0 | \Phi_i \rangle = E_i^0 | \Phi_i \rangle . \tag{6}$$

R denotes the residual interaction.

The exact eigenstates $|\Psi_i\rangle$ of H_N can be represented by a perturbation expansion

$$|\Psi_i\rangle = |\Phi_i\rangle + [R/(E_i - H_0)] |\Psi_i\rangle . \tag{7}$$

In the following we want to discuss only first order effects of the nucleon-nucleon forces; i.e., we use

$$|\Psi_i\rangle = |\Phi_i\rangle + [R/(E_i - H_0)] |\Phi_i\rangle \tag{8}$$

(generalization to higher NN correlations is straightforward). The transition matrix M_{fi}, Eq. (1), is then given by (A denotes the number of particles):

$$M_{fi} = \langle A - j; j | H_{el} | A \rangle \tag{9}$$

$$= \langle \Phi_f | H_{el} | \Phi_i \rangle \tag{9a}$$

$$+ \left\langle \Phi_f \left| \frac{R}{E_f - H_0} H_{el} \right| \Phi_i \right\rangle \tag{9b}$$

$$+ \left\langle \Phi_f \left| H_{el} \frac{R}{E_i - H_0} \right| \Phi_i \right\rangle . \tag{9c}$$

Given the "correct" electromagnetic interaction H_{el}, the transition matrix can be calculated by Eq. (9). How does this electromagnetic interaction look for our system (interaction V)? Without nucleon-nucleon interactions we know the answer already. In this case, H_{el} is a sum of one-body operators given by

$$H_{el} = \sum_{\alpha = 1}^{A} h_{el}(\alpha) , \tag{10}$$

with

$$h_{el}(\alpha) = \vec{A} \cdot \vec{p}/M . \tag{11}$$

$\vec{A}$ denotes the vector potential of the photon. We

consider in the following only the electric contributions to $h_{el}(\alpha)$ in the approximation

$$h_{el}(\alpha) = [H_0, Q_L(\alpha)] . \tag{12a}$$

Here $Q_L(\alpha)$ are the usual electric operators

$$Q_L(\alpha) = \{e_L^{eff}(p)\tfrac{1}{2}[1 + \tau^3(\alpha)] + e_L^{eff}(n)\tfrac{1}{2}[1 - \tau^3(\alpha)]\}$$

$$\times \frac{1}{k_\gamma}\left(1 + r\frac{d}{dr}\right) j_L(k_\gamma r)Y_L^\mu(\hat{r}) . \tag{12b}$$

Using this electromagnetic interaction (one-body operator) our transition matrix Eq. (9) is not gauge invariant. In Fig. 2 we show the contributions taken into account by the use of a one-body operator H_{el}. Figure 2(a) corresponds to the expression Eq. (9a): pure shell model–no correlations; Figs. 2(b) and 2(c) correspond to the expression Eq. (9b): final state correlations, Figs. 2(d) and 2(e) correspond to the expression Eq. (9c): initial state correlations. In all these processes the photon interacts only with external nucleon lines (i.e. positive energy states). As already mentioned, introducing correlations in this way does not insure gauge invariance of the transition matrix. From the requirement of gauge invariance the additional pieces to Eq. (9) can be obtained. We do not want to discuss this in detail as it is already discussed in the literature.[7-10] The processes required by gauge invariance are shown in Fig. 3. We see that these

processes correspond to the interaction of the photon with internal nucleon lines, exchanged mesons, and intermediate nucleons in other than positive energy states. These additional exchange contributions are given [in the approximation of Eq. (12)] by:

$$M_{int} = \langle \Phi_f | [V, Q_L] | \Phi_i \rangle . \tag{13}$$

The total transition matrix M_{fi} is thus given by

$$M_{fi} = M^{sm} + M_{ext}^f + M_{ext}^i + M_{int} , \tag{14}$$

where M^{sm} denotes the shell model contribution, M_{ext}^f and M_{ext}^i denote the NN correlation contributions (final and initial state), and M_{int} the internal or meson exchange contributions. We shall now discuss the different parts of the transition matrix M_{fi} separately.

A. Shell model

The shell model contribution is given by

$$M^{sm} = \langle \Phi_f | H_{el} | \Phi_i \rangle$$
$$= \langle \Phi_f | [H_0, Q_L] | \Phi_i \rangle \tag{15}$$
$$= (E_f^0 - E_i^0)\langle \Phi_f | Q_L | \Phi_i \rangle$$
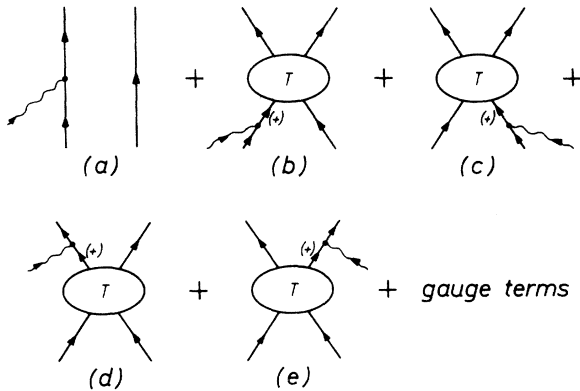
(note that Q_L is a long range operator).

FIG. 2. Different contributions to the total transition matrix M_{fi}. T is the T matrix arising from the residual interaction R. The calculations in this paper are performed in the approximation $T = R$. The total transition matrix M_{fi} is separated into the following pieces: (a) photon interaction in the pure shell model, (b) and (c) photon interaction with the nucleons before the nucleon-nucleon interaction (final state correlation), (d) and (e) photon interaction with the nucleons after the nucleon-nucleon interaction occurs (initial state correlation). The + sign in diagrams (b)–(e) denotes positive energy solutions; i.e., shell model states.
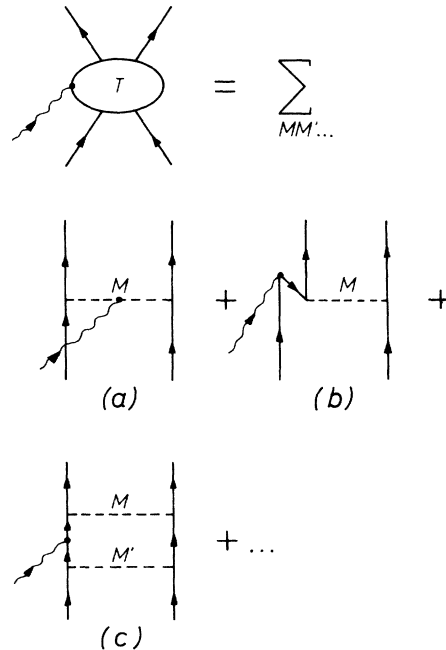

FIG. 3. Gauge terms to the total transition matrix M_{fi}. M denotes the exchanged mesons.

B. Final state correlations

The contribution from the final state correlation
is given by (diagram, Fig. 4):

$$M_{ext}^f = \left\langle \Phi_f \left| \frac{R}{E_f - H_0} [H_0, Q_L] \right| \Phi_i \right\rangle \tag{16}$$

$$= \sum_n \left\langle \Phi_f \left| \frac{R}{E_f - E_n^0} \right| n \right\rangle \langle n|[H_0, Q_L]|\Phi_i\rangle . \tag{17}$$

Evaluating the commutator we obtain

$$M_{ext}^f = \sum_n \frac{E_n^0 - E_i^0}{E_f - E_n^0} \langle \Phi_f|R|n\rangle\langle n|Q_L|\Phi_i\rangle \tag{18}$$

or, with the photon energy $E_\gamma \equiv E_f$ and $E_i^0 \equiv 0$,

$$M_{ext}^f = \sum_n \left(-1 + \frac{E_\gamma}{E_\gamma - E_n^0}\right)\langle\Phi_f|R|n\rangle\langle n|Q_L|\Phi_i\rangle . \tag{19}$$

The calculation of the matrix element Eq. (19) can
be considerably simplified in a good approximation
by using closure to the multipole states. This has
been done earlier by Brown in the reactions (n, γ)
and (p, γ) just above the dipole resonance region.[11]
Similar expressions have been used by Fujii and
Sugimoto.[12] As we are interested in the region of
photon energy $E_\gamma > 50$ MeV this is the best way to
take into account the coupling to the resonance
modes. (This should not really be considered as
an approximation; it avoids the use of effective
charges arising from the coupling to the resonance
modes.) Denoting by ΔE_L a characteristic transi-
tion energy (dipole: $\Delta E_1 \sim \hbar\omega$, quadrupole: ΔE_2
$\sim 2\hbar\omega$) we obtain from Eq. (19):

$$M_{ext}^f = \left(-1 + \frac{E_\gamma}{E_\gamma - \Delta E_L}\right)\langle\Phi_f|RQ_L|\Phi_i\rangle. \tag{20}$$

For increasing photon energy E_γ this contribution
becomes less important as

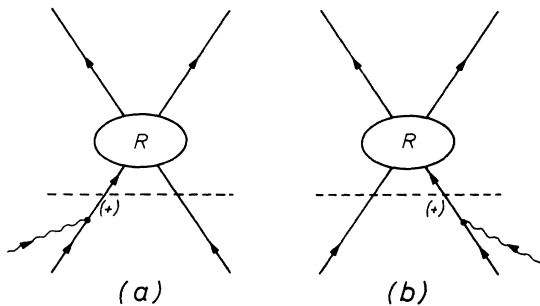$$\lim_{E_\gamma \to \infty} \left(-1 + \frac{E_\gamma}{E_\gamma - \Delta E_L}\right) \to 0 . \tag{20a}$$

C. Initial state correlations

In a similar way, using closure to the electric
multipole states, we obtain the following expression
for M_{ext}^i (diagram, Fig. 5):

$$M_{ext}^i = \left(1 - \frac{E_\gamma}{E_\gamma + \Delta E_L}\right)\langle\Phi_f | Q_L R|\Phi_i\rangle . \tag{21}$$

Also, the contributions from initial state correla-
tions tend to zero for increasing photon energy:

$$\lim_{E_\gamma \to \infty} \left(1 - \frac{E_\gamma}{E_\gamma + \Delta E_L}\right) \to 0 . \tag{22}$$

We see that both contributions to the transition
matrix arising from the NN correlations—final
state as well as initial state correlations—become
less important for increasing energy E_γ.

D. Exchange contributions

The exchange contributions (Figs. 6 and 7) are
given by

$$M_{int} = \langle\Phi_f |[V, Q_L]|\Phi_i\rangle . \tag{23}$$

A remarkable fact concerning this contribution
is that it does not show such a dramatic dependence
on the photon energy as the initial and final state
correlations [Eqs. (20) and (21)]. For energies
E_γ near the pion threshold these processes clearly
seem to dominate the photonuclear reactions. The
numerical example we shall consider in Sec. III
manifests these facts. We shall see in the following
that the isospin dependence of this interaction
operator explains the successful working of the
quasideuteron model. The isospin dependence
of the commutator is of the form

$$[V, Q_L] \sim (\vec{\tau}_1 \times \vec{\tau}_2)_z \sim \tau_1^+\tau_2^- - \tau_1^-\tau_2^+ , \tag{24}$$

which indicates that the contributions M_{int} are

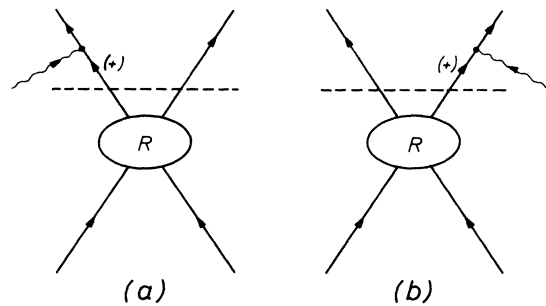FIG. 4. Final state correlations in first order of the
residual interaction R.

FIG. 5. Initial state correlations in first order of the
residual interaction R.

symmetric in effect for neutrons and protons:

$$(\tau_1^+\tau_2^- - \tau_1^-\tau_2^+)|np\rangle = |pn\rangle \ ,$$

$$(\tau_1^+\tau_2^- - \tau_1^-\tau_2^+)|pp\rangle = 0 \ , \qquad (25)$$

$$(\tau_1^+\tau_2^- - \tau_1^-\tau_2^+)|nn\rangle = 0 \ .$$

Concerning the photonuclear reactions this means that the exchange contributions to (γ, n) and (γ, p) are equally important. For (γ, pn) reactions M_{int} does contribute while for (γ, pp) and (γ, nn) we obtain *no* contribution. For these reactions only the initial and final state correlations are possible (less important for increasing energies).

It is interesting to discuss the reason for the relative suppresion of the reactions (γ, pp) and (γ, nn) compared to the reaction (γ, pn). Considering for simplicity the exchange of one pion only, we show the processes contributing to (γ, pn) in Fig. 6. For charged pion exchange, only diagrams (a) and (c) can contribute to the electric process. Diagram Fig. 6(b) gives no contribution. For (γ, pp) and similarly for (γ, nn) (Fig. 7), both diagrams (a) and (b) can contribute; however, because of different time ordering the contributions cancel each other. Process diagram Fig. 7(c) gives no contribution as a neutral particle is exchanged. It should be noted that according to the

gauge invariance of our description, the Siegert theorem is not violated as can be seen from the total transition matrix in the form of Eqs. (15), (20), (21), and (23).

III. NUMERICAL EXAMPLE

In order to show the importance of the different contributions which altogether make up (in our description) the (γ, p) and (γ, n) process—shell model, correlation contributions (initial and final state), mesonic exchange contribution—we give numerical results for (γ, p) and (γ, n) on ^{4}He for photon energies $E_\gamma > 50$ MeV. [Calculations for $E_\gamma < 50$ MeV have been reported in the literature (Refs. 13–15). In this energy region our model is not suited for a detailed calculation, since by using closure to the dipole and quadrupole states one cannot expect reasonable results near the center of the multipole states.] We know from Eqs. (20), (21), and (23) that the treatment of short range correlations is not of great importance (note that Q_L is a long range operator). This
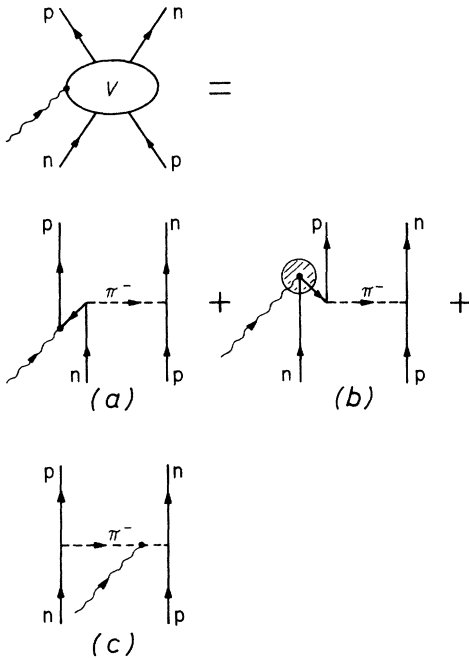

FIG. 6. Exchange contributions to the interaction of a photon with the neutron-proton system. Only diagrams (a) and (c) give essential contribution to the electric interaction. Diagram (b) does not contribute.
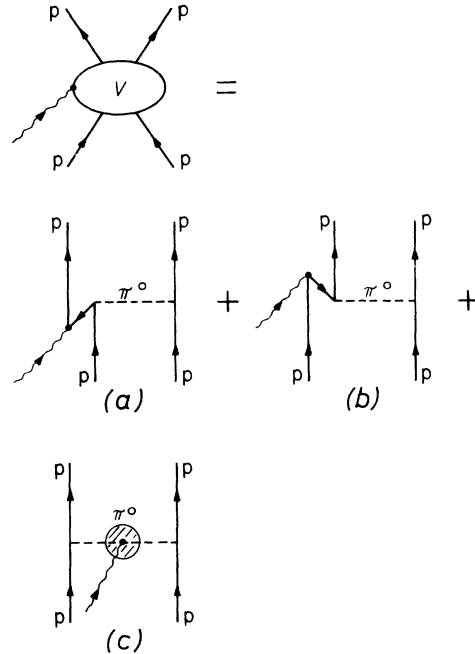

FIG. 7. Exchange contributions to the interaction of a photon with a proton-proton system. Both diagrams (a) and (b) give contributions to the electric interaction of a photon with a proton pair. However, because of different time ordering both diagrams cancel. Diagram (c) gives no contribution as a neutral pion is exchanged. The cancellation of diagrams (a) and (b) leads to a strong suppression of the reaction (γ, pp) compared to the reaction (γ, pn). The suppression of (γ, nn) has an equivalent reason.

allows us to obtain good numerical results with
the use of an effective nucleon-nucleon potential.
It should be noted also that the use of an effective
potential does not destroy our arguments about
the gauge invariance of the transition matrix.
From the above arguments we expect only the long
range part of the potential to be important. Con-
cerning the electromagnetic operators we take
into account only electric dipole and quadrupole
interactions, which is a very good limit.

In the preceding section the following expression
for the transition matrix was derived:

$$M_{fi} = E_\gamma \langle \Phi_f | Q_L | \Phi_i \rangle \tag{26a}$$

$$+ \left(-1 + \frac{E_\gamma}{E_\gamma - \Delta E_L} \right) \langle \Phi_f | R Q_L | \Phi_i \rangle \tag{26b}$$

$$+ \left(1 - \frac{E_\gamma}{E_\gamma + \Delta E_L} \right) \langle \Phi_f | Q_L R | \Phi_i \rangle \tag{26c}$$

$$+ \langle \Phi_f | [V, Q_L] | \Phi_i \rangle . \tag{26d}$$

In our example a single nucleon (neutron or proton)
is emitted from a single particle state $|k\rangle$ into
a continuum state $|a\rangle$. The transition matrix Eq.
(26) is evaluated as follows:

$$M_{fi} = E_\gamma \langle a | Q_L | k \rangle + \left(-1 + \frac{E_\gamma}{E_\gamma - \Delta E_L} \right) \sum_\nu \langle a(1)\nu(2) | V(1,2)\{Q_L(1) + Q_L(2)\} | k(1)\nu(2) - \nu(1)k(2) \rangle$$

$$+ \left(1 - \frac{E_\gamma}{E_\gamma + \Delta E_L} \right) \sum_\nu \langle a(1)\nu(2) | \{Q_L(1) + Q_L(2)\} V(1,2) | k(1)\nu(2) - \nu(1)k(2) \rangle$$

$$+ E_\gamma \left[\frac{1}{E_\gamma - \Delta E_L} - \frac{1}{E_\gamma + \Delta E_L} \right] \left[-\langle a | U Q_L | k \rangle + \sum_\nu \langle a | Q_L | \nu \rangle \left(-\sum_i \langle i\nu - \nu i | V | ik \rangle + \langle \nu | U | k \rangle \right) \right]$$

$$+ \sum_\nu \langle a(1)\nu(2) | [V(1,2), \{Q_L(1) + Q_L(2)\}] | k(1)\nu(2) - \nu(1)k(2) \rangle . \tag{27}$$

All states in this expression are eigenstates to
our model Hamiltonian H_0. For the present cal-
culation we have chosen a fixed Hamiltonian

$$H_0 = T + U , \tag{28}$$

where the single particle potential U is taken to be
of Woods-Saxon type:

$$U(r) = -62.0 \frac{1}{1 + \exp[(r - 1.74)/0.4]} \quad [\text{MeV}] \tag{29}$$

for both neutrons and protons. This potential is
chosen to give a binding energy of 20.7 MeV for
a nucleon in the $1s$ state.

The states $|\nu\rangle$, $|i\rangle$, and $|k\rangle$ are bound $1s$ states
The state $|a\rangle$ denotes the continuum state of the
outgoing particle (eigenstate of the same Hamilto-
nian H_0).

The nucleon-nucleon potential V is chosen as

$$V(r) = -V_0 (e^{-\mu r}/\mu r)[P_M + \tfrac{1}{4} P_\sigma] , \tag{30}$$

with $\mu = 0.71$ fm^{-1}. We use for V_0 three values:
36 MeV,[16] 44 MeV, and 60 MeV.

The effective charges in the operator Q_L are
listed in Table I. We note here that the choice of
these effective charges is not without problem.[17]
This effect, however, is of minor importance in

our calculations. We use the following values for
ΔE_L: $L = 1$, 22 MeV; $L = 2$, 33 MeV.

We have calculated both the angular distributions
and total cross sections for the reactions (γ, p)
and (γ, n). The angular distributions are evaluated
in the form ($E1$ and $E2$ only):

$$\frac{d\sigma}{d\Omega} (k_\gamma, \Theta) = \sum_{\lambda=0}^{4} C_\lambda(k_\gamma) P_\lambda(\cos\Theta) . \tag{31}$$

Here C_λ contains the transition matrix. The ex-
plicit form is given in the Appendix. Equivalently,
we can write for the angular distribution

$$\frac{d\sigma}{d\Omega} (k_\gamma, \Theta) = a + b \sin^2\Theta + c \cos\Theta$$

$$+ d \sin^2\Theta \cos\Theta + c \sin^2\Theta \cos^2\Theta , \tag{32}$$

TABLE I. Effective charges (dipole and quadrupole
case) for proton and neutron chosen in the numerical
calculation.

L	$e_L^{\text{eff}}(p)$	$e_L^{\text{eff}}(n)$
1	$\frac{1}{2}$	$-\frac{1}{2}$
2	$\frac{5}{8}$	$\frac{1}{8}$

where the coefficients are given in terms of C_λ:

$a = C_0 + C_2 + C_4$ = 0 in our calculation since no spin flip occurs,

$b = -\frac{3}{2}C_2 - \frac{5}{8}C_4$,

$c = C_1 + C_3$ = 0 in our calculation,   (33)

$d = -\frac{5}{2}C_3$,

$e = -\frac{35}{8}C_4$.

The ratios d/b (a measure for the asymmetry) and e/b (equal to $5\sigma_{E2}/\sigma_{E1}$) will also be compared with experimental data as far as available. Further, the integrated cross section is given by

$$\sigma(k_\gamma) = 4\pi C_0(k_\gamma) \ .$$ (34)

IV. RESULTS AND DISCUSSION

In Fig. 8 we show our results for the total cross section of $^4\text{He}(\gamma, p)^3\text{H}$. The contributions of the different pieces (in addition to the shell model) according to Eq. (26) are presented separately. Curve A shows the cross section obtained from the shell model matrix element, Eq. (26a). The
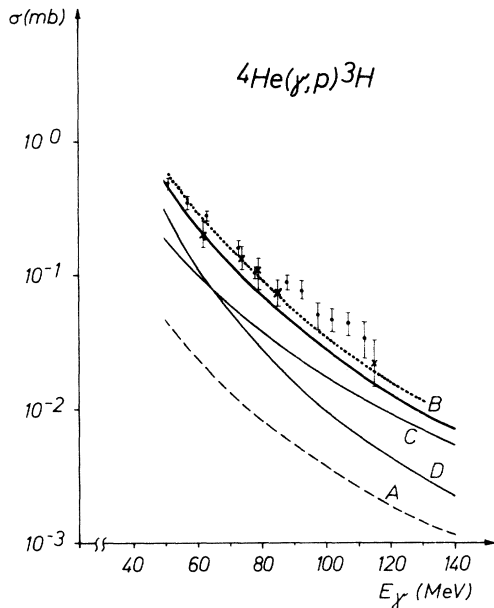

FIG. 8. Total cross section for the reaction (γ, p) on ^4He as a function of the photon energy E_γ. A—shell model contribution, C—shell model plus photon-meson exchange contribution, D—shell model plus nucleon-nucleon correlations, B—total transition matrix: shell model plus photon-meson exchange contributions plus nucleon-nucleon correlations. The given curves are calculated with a potential depth $V_0 = 44$ MeV. The dotted line belongs to the total cross section calculated with $V_0 = 60$ MeV. This indicates the dependence of the results on the nucleon-nucleon potential of use. Experimental data are taken from Ref. 18 ($\blacksquare$) and Ref. 19 ($\divideontimes$).

shell model cross section is about one order of magnitude smaller than the experimental one. This agrees with the observed trend in other nuclei.

In curve C we present the shell model contribution plus the main correction obtained from our model, namely the meson exchange contribution, Eq. (26d). From the discussion of Eq. (22) we expected that for higher energies this term will be dominant. In fact this shows up in the numerical example. The exchange contributions alone nearly explain the experimental data for energies above 80 MeV.

In curve D we discuss the effect of the nucleon-nucleon correlations in addition to the shell model. We obtain the expected trend. For higher energies these contributions become much less important than the gauge terms (curve C).

In curve B we show the integrated cross section obtained by the use of the full transition matrix, Eqs. (26a)–(26d). For our choice of the potential depth $V_0 = 44$ MeV the results are able to explain the experimental findings. Varying the potential depth gives us a feeling for the importance of having chosen the correct nucleon-nucleon potential. The dotted line corresponds to $V_0 = 60$ MeV. We see that the change of σ with the depth is not dramatic and that easily a value of V_0 can be chosen to achieve complete agreement with the experiments.

In Fig. 9 we present the results for the integrated cross section of the reaction $^4\text{He}(\gamma, n)^3\text{He}$. We have essentially the same behavior as for (γ, p), in Fig. 8. This is the reason for not discussing the different contributions again. We show the shell model contribution (curve A) and the cross section obtained for the total transition matrix for different values of the potential depth ($B_1 \equiv 36$ MeV, $B_2 \equiv 44$ MeV, and $B_3 \equiv 60$ MeV). The comparison with the experiment does not give too much insight into the physics, as there is not enough experimental information.

We turn now to the discussion of the angular distributions, Figs. 10 and 11. In Fig. 10 we compare the angular distributions of the reactions (γ, p) and (γ, n) for 60 MeV photon energy. The shell model contribution (curves A) shows a peak in forward direction for (γ, p) and a backward peak for (γ, n). The additional exchange contributions (curves C) already give the correct trend for both (γ, p) and (γ, n), namely a peak in the forward direction. The angular distributions calculated with the total transition matrix (shell model + correlations + gauge terms) are given by curves B. We see that the nucleon-nucleon correlations in addition enhance the forward asymmetry for (γ, n). The results are in agreement with the

experimental findings. The angular distribution of (γ, n) is found to be peaked less in forward direction than the one of (γ, p) which agrees too with the experiment.

In Fig. 11 we show the angular distribution for (γ, p) and (γ, n) for a photon energy of 100 MeV. Here we discuss two potential depths. Curves C_1, B_1 correspond to $V_0 = 36$ MeV, curves C_2 and B_2 correspond to $V_0 = 44$ MeV (curves C_i shell model + gauge term, curves B_i total transition matrix). An interesting fact is that the effect of the nucleon-nucleon potential is more pronounced in the angular distribution. This leaves a good possibility for the determination of the nucleon-nucleon potentials from measurements of the angular distributions.

For a more detailed discussion of the angular distributions we present the results in the form of Eq. (32). The ratios d/b and e/b are given in Table II for (γ, p) and in Table III for (γ, n) in comparison with experimental values as far as available. We have seen already that besides the total cross sections also the angular distributions are showing the main trend of the experimental data.

The ratio d/b which represents the angular asymmetry is in good agreement with the experimental data. We also obtain the observed trend
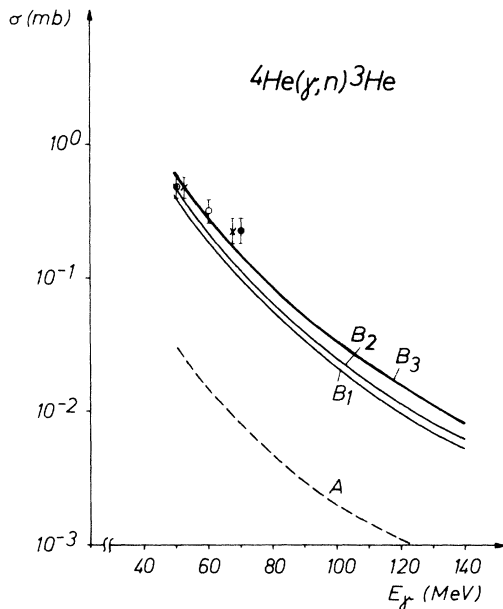
FIG. 10. Angular distributions of the reactions ^{4}He$(\gamma, p)^3$H and ^{4}He$(\gamma, n)^3$He for $E_\gamma = 60$ MeV. A—shell model calculations, C—shell model plus photon-meson exchange contribution, B—total transition matrix. $(V_0 = 36$ MeV$)$.

FIG. 9. Total cross section for the reaction (γ, n) on ^{4}He as a function of the photon energy E_γ. A—shell model contribution, B—total transition matrix as a function of the nucleon-nucleon potential used in the calculation $(B_1 = 36$ MeV, $B_2 = 44$ MeV, $B_3 = 60$ MeV$)$. Experimental data are taken from Ref. 19 ($\mathbf{\Phi}$) and Ref. 20 (ϕ).
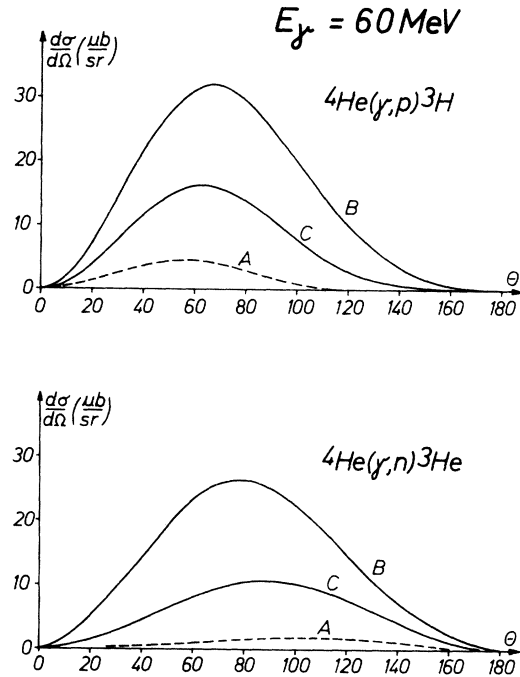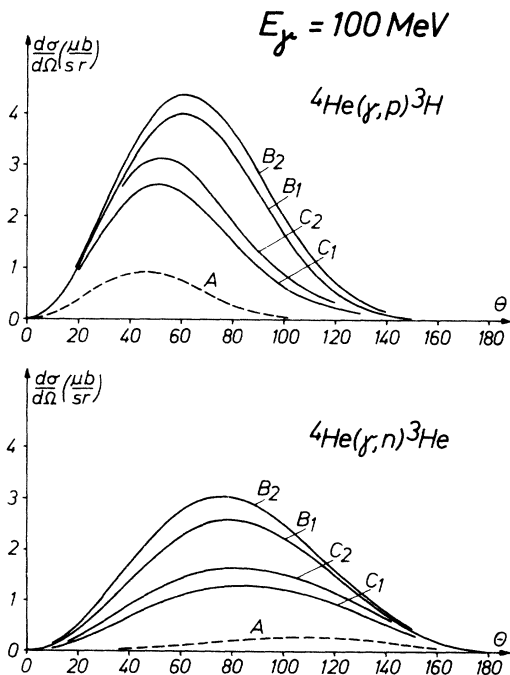
FIG. 11. Angular distributions of the reactions ^{4}He$(\gamma, p)^3$H and ^{4}He$(\gamma, n)^3$He for $E_\gamma = 100$ MeV. Same as Fig. 10 with potential depth $V_0 = 36$ MeV (C_1, B_1) and $V_0 = 44$ MeV (C_2, B_2).

TABLE II. Integrated cross sections and ratios d/b and e/b for the reaction (γ,p) on ^{4}He as a function of the photon energy E_γ.

E_γ (MeV)	$\sigma_{(\gamma,p)}$ (mb)	d/b Theor	d/b Exp [a,b]	$e/b = 5\sigma(E2)/\sigma(E1)$ Theor	$e/b = 5\sigma(E2)/\sigma(E1)$ Exp [a]
50	5.00×10^{-1}	0.73	0.6–1.0	0.22	0.4–0.9
60	2.28×10^{-1}	1.12	0.8–1.2	0.37	0.5–1.0
80	7.20×10^{-2}	1.50	0.9–1.4	0.62	0.8–1.3
100	2.80×10^{-2}	1.72	1.1–1.5	0.76	$\cdots$
120	1.32×10^{-2}	1.87	$\cdots$	0.90	$\cdots$
140	7.11×10^{-3}	1.96	$\cdots$	0.98	$\cdots$

[a] Reference 18.
[b] Reference 19.

TABLE III. Integrated cross sections and ratios d/b and e/b for the reaction (γ,n) on ^{4}He as a function of the photon energy E_γ.

E_γ (MeV)	$\sigma_{(\gamma,n)}$ (mb)	d/b Theor	d/b Exp [a]	$e/b = 5\sigma(E2)/\sigma(E1)$ Theor
50	4.85×10^{-1}	0.40	0.05–0.16	0.07
60	2.16×10^{-1}	0.45	0.12–0.30	0.06
80	6.55×10^{-2}	0.50	$\cdots$	0.06
100	2.47×10^{-2}	0.53	$\cdots$	0.07
120	1.15×10^{-2}	0.57	$\cdots$	0.08
140	6.16×10^{-3}	0.61	$\cdots$	0.10

[a] Reference 20.

of the asymmetry in dependence of the photon energy, namely an increase of the forward asymmetry with increasing photon energy. For (γ, n) our values of d/b appear to be somewhat larger than the experimental values.

The ratio e/b is a measure for the quadrupole contribution in the total cross section. Our values show the right trend with increasing photon energy. However, the values are somewhat too small. The reason for this can probably be found in the quadrupole transition energy chosen by us and seems not to be a failure of our method.

V. CONCLUSION

In the present paper we have discussed the dynamical aspects of photonuclear reactions. The transition matrix has been built up from the physical processes which enter the reactions. The contributions to the total transition matrix consist of three pieces: shell model contribution, nucleon-nucleon correlation parts in which the photon interacts with external nucleon states (positive energy states) and terms necessary to achieve gauge invariance of the description. This procedure has an advantage over the usual treatment via Siegert's theorem, insofar as the physical processes can be discussed separately, and as the contributions usually called short-range correlations are not mixed up with the correlations connected with the interaction of the photon with internal nucleons (negative energy states) or with mesons mediating the correlations.

We have shown that for energies starting below the pion threshold the gauge contributions to the nucleon-nucleon correlations (mostly not considered in calculations) gives the main contribution to the transition matrix. As this interaction is symmetric for neutrons and protons it gives the main contribution for (γ, pn) and does not con-

tribute for the same reason to the reactions (γ, pp) and (γ, nn). This leads to a strong suppression of these reactions compared to (γ, np). The correlations usually introduced are shown to be not as important as thought up to now.

For a numerical example we have chosen the reactions (γ, n) and (γ, p) on ^{4}He. The reason for taking ^{4}He in a model calculation has been for simplicity only. For the same reason an effective potential has been chosen. For heavier nuclei the arguments are valid in the same way. Our results obtained for (γ, p) and (γ, n) are in over-all good agreement with the experiments. We have been able to explain the total cross sections for (γ, n) and (γ, p) as well as the angular distributions. The effect of the photon-meson contributions has been shown to be dominant for photon energies $E_\gamma > 80$ MeV. The short range correlations in the usual sense are less important in this energy region. In conclusion we remark that the presented model is expected to explain the experimental findings of (γ, p), (γ, n), and (γ, pn) reactions in heavier nuclei as well.

APPENDIX: EXPLICIT FORM OF THE ANGULAR DISTRIBUTION FOR (γ, p) AND (γ, n) REACTIONS ON ^{4}He

The single particle states $|k\rangle$ and $|a\rangle$ entering Eq. (27) have the following orbital parts:

$$\langle \vec{r} | k \rangle = \zeta_k(\vec{r}) = \frac{1}{r} R(r) Y_0^0(\hat{r}) , \qquad (A1)$$

$$\langle \vec{r} \,|\, a \rangle = \psi_{\vec{k}_a}^{(-)}(\vec{r}) = \sum_{l_a,\nu} 4\pi i^{\,l_a} e^{-i\,\delta_{l_a}} \zeta_{l_a}(k_a,r) Y_{l_a}^{\nu}{}^{*}(\hat{k}_a) Y_{l_a}^{\nu}(\hat{r}) \, , \tag{A2}$$

$$\zeta_{l_a}(k_a,r) \xrightarrow[r\to\infty]{} \frac{1}{k_a r}\sin(k_a r - \tfrac{1}{2}l_a\pi + \delta_{l_a}) \, . \tag{A3}$$

The angular distribution is written in the form of Eq. (31). In our calculation $C_\lambda(k_\gamma)$ is given by

$$C_\lambda(k_\gamma) = -2\,\frac{e^2 M_{\text{red}}}{\hbar^2} k_a k_\gamma \sum_{L,\bar{L}=1}^{2} \frac{(2L+1)(2\bar{L}+1)}{[L(L+1)\bar{L}(\bar{L}+1)]^{1/2}} (L0\bar{L}0\,|\,\lambda 0)\,(L1\bar{L}-1\,|\,\lambda 0)\cos(\delta_\lambda - \delta_{\bar{\lambda}})\Re_L(k_\gamma)\Re_{\bar{L}}(k_\gamma) \, . \tag{A4}$$

$M_{\text{red}} = \tfrac{3}{4}M$ equals the reduced mass of the outgoing nucleon and the residual nucleus. The wave number k_a is related to $E_\gamma = \hbar c k_\gamma$ and the separation energy B of the emitted nucleon by

$$\hbar^2 k_a^2 / 2 M_{\text{red}} = E_\gamma - B \, . \tag{A5}$$

$\Re_L(k_\gamma)$ is given by

$$\Re_L = e_L^{\text{eff}}(J_L + \Omega_L) + \kappa_L K_L + \delta_{2L}\Gamma_L \, , \tag{A6}$$

where

$$\kappa_{L=1} = \begin{cases} +1 \text{ for protons} \\ -1 \text{ for neutrons} \end{cases} \quad \text{and} \quad \kappa_{L=2} = \begin{cases} +\tfrac{1}{2} \text{ for protons} \\ -\tfrac{1}{2} \text{ for neutrons} \end{cases}$$

The expressions J_L, Ω_L, K_L, and Γ_2 are defined as

$$J_L(k_\gamma) = \left\{ 1 + (0.9V_0 - 39.4)\left(\frac{1}{E_\gamma - \Delta E_L} - \frac{1}{E_\gamma + \Delta E_L}\right) \right\} \int_0^\infty dr\,r\,\zeta_L(k_a,r)g_L(k_\gamma,r)R(r) \, , \tag{A7}$$

$$\Omega_L(k_\gamma) = -\left(\frac{1}{E_\gamma - \Delta E_L} - \frac{1}{E_\gamma + \Delta E_L}\right)\int_0^\infty dr\,r\,\zeta_L(k_a,r)U(r)g_L(k_\gamma,r)R(r) \, , \tag{A8}$$

$$K_L(k_\gamma) = \int_0^\infty dr\,r\,\zeta_L(k_a,r)G_L(k_\gamma,r)R(r) \, , \tag{A9}$$

$$\Gamma_L(k_\gamma) = \int_0^\infty dr\,r\,\zeta_L(k_a,r)H_L(k_\gamma,r)R(r) \, . \tag{A10}$$

$g_L(k_\gamma,r)$ is the radial part of the operator Q_L, see Eq. (12b):

$$g_L(k_\gamma,r) = \frac{r}{2L+1}\left\{(L+1)j_{L-1}(k_\gamma r) - L j_{L+1}(k_\gamma r)\right\}. \tag{A11}$$

For our choice of the potential V, Eq. (30), the quantities G_L and H_L are given by

$$G_L(k_\gamma,r) = \frac{1}{16\pi}\int_0^\infty dr_1 R^2(r_1)\left[\left(\frac{5}{E_\gamma - \Delta E_L} + \frac{3}{E_\gamma + \Delta E_L}\right)v_L(r,r_1)g_L(k_\gamma,r_1)\right.$$

$$\left. -\left(\frac{2}{E_\gamma - \Delta E_L} + \frac{6}{E_\gamma + \Delta E_L}\right)v_0(r,r_1)g_L(k_\gamma,r)\right] \, , \tag{A12}$$

$$H_L(k_\gamma,r) = \frac{9}{32\pi}\left(\frac{1}{E_\gamma - \Delta E_L} - \frac{1}{E_\gamma + \Delta E_L}\right)\int_0^\infty dr_1 R^2(r_1)[v_L(r,r_1)g_L(k_\gamma,r_1) + v_0(r,r_1)g_L(k_\gamma,r)] \, . \tag{A13}$$

v_0 and v_L arise from the expansion of our potential V in the form

$$-V_0\,\frac{\exp(-\mu r_{12})}{\mu r_{12}} = \sum_{\Lambda,\kappa} v_\Lambda(r_1,r_2)Y_\Lambda^{\kappa}{}^{*}(\hat{r}_1)Y_\Lambda^{\kappa}(\hat{r}_2) \, . \tag{A14}$$

In this special case we have

$$v_\Lambda(r_1,r_2) = 4\pi V_0 \begin{cases} h_\Lambda^{(1)}(i\mu r_1)j_\Lambda(i\mu r_2) & r_1 > r_2 \, , \\ j_\Lambda(i\mu r_1)h_\Lambda^{(1)}(i\mu r_2) & r_1 < r_2 \, . \end{cases} \tag{A15}$$

[1]M. Fink, H. Hebach, and H. Kümmel, Nucl. Phys. A186, 353 (1972).

[2]W. Weise and M. G. Huber, Nucl. Phys. A162, 301 (1972).

[3]G. M. Shklyarevskii, Sov. Phys.—JETP 14, 324 (1962).

[4]A. Malecki and P. Picchi, Nuovo Cimento Lett. 8, 16 (1973).

[5]J. S. Levinger, Phys. Rev. 84, 43 (1951).

[6]M. Gari and H. Hebach, Phys. Lett. 49B, 29 (1974).

[7]L. L. Foldy, Phys. Rev. 92, 178 (1953).

[8]R. G. Sachs and N. Austern, Phys. Rev. 81, 705 (1951).

[9]M. Gari and A. H. Huffman, Phys. Rev. C 7, 531 (1973).

[10]M. Gari and A. H. Huffman, U. S. Atomic Energy Commission Research and Development Report No. Calt 63-164 (unpublished).

[11]G. E. Brown, Nucl. Phys. 57, 339 (1964).

[12]S. Fujii and O. Sugimoto, Nucl. Phys. 56, 73 (1964).

[13]J. Hüfner and C. M. Shakin, Phys. Rev. 175, 1350 (1968).

[14]F. Beck and A. Müller-Arnke, Phys. Lett. 27B, 343 (1968).

[15]L. Crone and C. Werntz, Nucl. Phys. A134, 161 (1969).

[16]D. Kurath, Phys. Rev. 101, 216 (1956).

[17]H. G. Miller and H. Arenhövel, Z. Phys. 249, 327 (1972).

[18]Yu. M. Arkatov, P. I. Vatset, V. I. Volshchuk, V. V. Kirichenko, I. M. Prokhorets, and A. F. Khodyachikh, Sov. J. Nucl. Phys. 12, 123 (1971).

[19]A. N. Garbunov, JETP Lett. 8, 88 (1968).

[20]D. V. Webb, C. K. Malcolm, Y. M. Shin, and D. M. Skopik, in Proceedings of the International Conference on Photonuclear Reactions and Applications, Asilomar, 1973, edited by B. L. Berman (Lawrence Livermore Laboratory, Univ. of California, Livermore, 1973), Vol. 2, Contribution 2B3.